Measurement of the screening potential in ^{3}H β decay

C. K. Hargrove
Centre for Research in Particle Physics, Carleton University, 1125 Colonel By Drive, Ottawa, Canada K1S 5B6

D. J. Paterson and I. S. Batkin
Ottawa-Carleton Institute for Physics, Physics Department, Carleton University, 1125 Colonel By Drive, Ottawa, Canada K1S 5B6

(Received 11 September 1998; published 9 August 1999)

A gas proportional chamber has been employed to make precise observations of the low-energy portion of the ^{3}H β spectrum in methane molecules. This spectrum has been well fit to the combination of an electron screening potential of 76 ± 4 (stat) ±9 (sys) eV, simultaneously with -22 ± 3 (stat) ±9 (sys) eV of molecular neutralization energy recovered in ionization of the gas. Both of these values are consistent with expectations based on self-consistent field predictions. [S0556-2813(99)02309-2]

PACS number(s): 23.40.−s

I. INTRODUCTION

The ^{3}H β-decay spectrum has been a frequent subject for study, combining the advantages of a simple nucleus within a minimal electron cloud and low decay energy ($\sim$18.6 keV) relative to that typical of other β decays. It is an allowed transition according to selection rules, thus having a relatively short lifetime so that high activity is easily achieved. It has been the primary choice for spectrum end-point studies in searches for evidence of neutrino mass [1,2]. It has also recently been the subject of attempts to observe discontinuities in the shape of the spectrum in pursuit of evidence for heavy neutrinos. A small ($\sim$1%) heavy neutrino component, with a mass near 17 keV, was suspected as a consequence of the studies of the ^{3}H spectrum by Simpson [3], apparently supported in studies made by other researchers [4–8] employing isotopes of heavier elements. In these studies, discontinuities in the slopes of the spectra of β-particle energies were observed to occur at points near 17 keV below the end-point energies for the isotopes under study. This support proved not to be robust in the other isotopes being studied, and the 17 keV neutrino was excluded at levels below $\frac{1}{2}$%. However, the careful ^{3}H observations of Simpson have not yet been understood.

One of the uncertain factors in the analysis of the heavy neutrino experimental results is an approximation in the β-decay theory. This approximation, by Rose [9], makes a correction to the predicted shape for the reduction in strength of the Coulomb field of the nucleus as seen by the escaping β particle due to the shielding of the nuclear charge by the cloud of bound electrons. This is the *screening* effect. To make this correction, a further approximation is made by assuming that the daughter atom suddenly has the atomic orbital structure of the parent. These approximations are generally believed to result in an inaccuracy in the theoretical spectrum at energies of less than $\sim$1 keV, depending upon the isotope being studied. Unfortunately, studies generally have not attempted to test the validity of these approximations even at such energies, due to the difficulties inherent in gathering reliable high statistics observations in this energy region, where detector systematic difficulties and environmental effects will dominate [10–12]. Even at higher energies, these factors can alter the theoretical prediction of the spectrum by a few percent. The screening potential is calculable, but requires a theoretical determination of the final-state probabilities for the atomic or molecular electron structure. Possible final states for the β decay of the tritium atom include the initial orbital electron being found in the ^{3}He ground state, or one of the possible excited states (*shake-up*), or the atom may be doubly ionized (*shake-off*). In the case where the tritium is bound in a molecule, these final-state probabilities are altered. In predicting the energy spectrum, all such final states are considered through corrections to the predicted energy of the escaping β particle in recognition of the depth of the well from which the β particle must escape prior to observation by a spectrometer. Adjustments are also made to the energy liberated in the decay to account for chemical energy changes in the decay. The above-mentioned searches for evidence of massive neutrinos concentrated on the electron spectra above the $\sim$1 keV region, which loosely defines a boundary for the region of validity of these approximations, though the absolute magnitude of these corrections was a matter of some theoretical discussion following Simpson's observations [13–15].

This work makes high precision studies of the ^{3}H β-decay energy spectrum, employing a gas proportional chamber [16]. The advantages of this method are its calorimetric nature, its simplicity, and its good resolution at the ^{3}H β energies. Our data collection runs have typically 10^8 decays each. This provides us with 1σ statistical uncertainties of $\sim$0.3% in each analog-to-digital converter channel between $\sim$1 and $\sim$5 keV. Background rates have been carefully measured to be 2% of the data rate, distributed similarly to the ^{3}H spectrum. The uncertainty in the background subtraction is less than 0.11% of the observations.

For this work, Monte Carlo simulations have predicted that about 0.45% of the β particles will encounter the detector walls, and that the observed energy distribution of such events will not greatly distort the overall spectrum. One concern of this method is that the wall effects are not readily monitored. Since the predicted level of wall effects is not verifiable, the actual wall effect rate is a free parameter in the fitting of the experimental data to the theory. The shape of the distortion due to wall effects is also not observable, and

is fixed for fitting purposes to that predicted by the Monte Carlo simulations.

In this work we measure the screening potential for the ^{3}H decay. This paper will discuss the theory of β decay and the associated final-state and environmental effects in Sec. II, and the observations and analysis in Sec. III. Conclusions will be drawn from our results in Sec. IV.

II. BETA DECAY

For allowed β decays, the nuclear matrix element does not depend on the lepton wave function. This permits us to employ a simplification in which summation of the squared matrix elements over all final states and spin states will yield a constant. The recoil energy of the nucleus may be neglected, since the maximum recoil energy is given simply as

$$E_{r,\max}=\left(\frac{m_e}{M_{\rm nucl}}\right)\times E_{e,\max}$$

For atomic tritium, $E_{e,\max}$ is $\sim$18.6 keV, yielding $\sim$3 eV for $E_{r,\max}$, which will not produce ionization. The distribution of β-particle energies (considering Coulomb interactions) is described via

$$P(E_e)dE_e=C' p_e E_e (E_0-E_e)^2 F(Z_f,E_e)dE_e. \qquad (1)$$

The spectrum is normalized via the constant C', E_0 is the energy released in the decay, E_e is the β-particle energy, $E_0-E_e=E_\nu$ where E_ν is the neutrino energy, and $F(Z_f,E_e)$ introduces a Coulomb correction factor, known as the Fermi function. This function of the β-particle energy and the charge Z_f of the daughter nucleus is given by [17,18]

$$F(Z_f,E_e)=2(1+s)(2p\rho)^{2s-2}e^{\pi\eta}\frac{|\Gamma(s+i\eta)|^2}{|\Gamma(2s+1)|^2},$$

where $\rho=R/(\hbar/mc)$, R is the nuclear radius, p is the β particle momentum in units of mc, $\eta=-\alpha Z_f/\beta$, α is the fine-structure constant, β is the relativistic particle velocity in units of c, and $s=[1-(\alpha Z_f)^2]^{1/2}$.

A. Radiative corrections

Radiative corrections to the β-particle energy spectrum are attributed to real or virtual photon emission or absorption by the β particle or the parent particle undergoing decay. Corrections involving one real or virtual photon vertex have a strength proportional to α. Corrections which involve two vertices have a strength proportional to α^2.

While it is anticipated that some of the decay energy will take the form of real photons in the detector (e.g., bremsstrahlung photon emission), for this detector such photons will be largely converted into ionization. Our analysis of these corrections concludes that they will occur at a level of only 10^{-4} in the β spectrum, and that partial recovery of the real photons in the gas will result in only a small effect, at the 10^{-5} level, on the predicted shape of the spectrum. All other radiative corrections affect only the normalization of the distribution. Since we anticipate an experiment which has systematic and statistical precisions of order $\sim$0.3% each, we may therefore safely neglect radiative corrections.

B. Screening of β particles by orbital electrons

Rose's method to incorporate the effect on the β spectrum [9] of screening of the nuclear charge by the orbital electron cloud involved the use of the WKB approximation method for describing the electron wave function in the nuclear potential well. This method simplifies to a calculation of the energy probability distribution for the β particles originating in the potential wells which are due to the probable final states of the orbital electrons. In light atoms such as ^{3}H, there is a large probability for shake-up of orbital electrons during β decay, leading to a range of possible final states and a corresponding range of screening potentials. The WKB method is valid in cases where the well depth is small relative to the particle energy. We will consider that a well depth $\sim\frac{1}{10}$th or less of the β particle energy satisfies this criterion. This will prove to place a lower limit, for the purposes of this work, on the reliable energy spectrum at $\sim$800 eV. According to Rose's method, the β-particle energy distribution is given as

$$P(E_e)dE_e=C' p'_e E'_e (E_0-E_e)^2 F(Z_f,E'_e)dE_e, \qquad (2)$$

where $E'_e=E_e-V_s$, and V_s is the screening potential.

In this section, we will consider the screening potential in the decay of an isolated tritium atom. The additional effects which can be predicted for the decay of tritium within a molecule will subsequently be considered in Sec. II C.

Shake-up and shake-off effects on screening

We begin by assuming that the velocity of the β particle is large relative to that of the orbital electrons (the *sudden approximation*) [19]. This implies that a decaying ^{3}H atom instantaneously transforms to the daughter ^{3}He atom, with the orbital electron cloud populating the ^{3}He orbitals in proportions given by the overlap between the original ^{3}H orbital and those of the ^{3}He atom. The overlap between the initial orbital and the various possible final states governs the probability for any particular final state, and determines the weight of the contributions of these instantaneous states to the screening potential. For atomic ^{3}H decay, the spherically symmetric initial and final orbital electron wave functions are sufficiently described by their radial parts as found in numerous texts on quantum physics [20], with $Z_i=1$, $Z_f=2$.

Taking the ^{3}H ground state as the initial state, overlap integrals are evaluated for final states including at least the ground state and the lowest three excited states of the daughter ^{3}He (with $\delta_{l,l'}$ always 0 for $l'\neq 0$). Then

$$\alpha_n=\left|\int_0^\infty dr\, R_{1,0}(r)_{(^3\mathrm{H})} r^2 R_{n,0}(r)_{(^3\mathrm{He})}\right|^2. \qquad (3)$$

The α_n shown in Table I thus determines the probabilities for shake-up to various final states, and completeness requires that the shake off probability is equal to one minus the

TABLE I. ^{3}H β-decay shake-up/shake-off probabilities, and screening potentials. The overlap probabilities, chemical energy shifts, and orbital excitation energy predictions are given for the β decay of atomic ^{3}H, for various excited levels of the daughter atom.

Final state ($^3He_n^{(*)}$)	Transition probability (α_n)	Energy shift (eV)	Excitation energy (eV)
$n=1$	0.7023	−54.46	0.0
$n=2$	0.2504	−13.52	−40.94
$n=3$	0.0131	−6.02	−48.44
$n=4$	0.0040	−3.39	−51.07
$^3He^{2+}$	0.0302	0.0	−54.46
Weighted sum	1.0000	−41.73	−12.73

summed shake-up probabilities. For each of these possible final states, according to the Rose approximation, the effect of screening is best incorporated by introducing a change in the distribution of β particle energies which reflects the effect of the potential well for the β-particle birth location, assumed to be at the center of the nucleus. This is simply the potential at the center of the nucleus for the orbital electron, calculated according to

$$V_n(0)=\int_0^\infty r^2\,dr\,R_{n,0}(r)_{(^3\mathrm{He})}\left(\frac{e^2}{r}\right)R_{n,0}(r)_{(^3\mathrm{He})}. \qquad (4)$$

This yields the energy shift results shown in the third column of Table I. These are weighted by the shake-up and shake-off probabilites (α_n) shown in the second column of Table I, for the final states (n) listed in the first column, in arriving at the mean energy shift (screening potential) at the bottom of the third column. The mean energy taken up into excitation of the orbital electron is given in the fourth column.

C. Consideration of molecular effects

It is not practical to maintain ionized or neutral atomic tritium in our detector, and so we chose a tritiated molecule to introduce the unstable element into our experiment. There will be small but significant effects on the spectrum due to changes in molecular binding and excitation which result from the nuclear decays. We now include these molecular rearrangements into our theoretical considerations.

We employ tritiated methane (CH_3T), called methyl tritium, in the detector. There are particular advantages in this choice. One small advantage rests in the fact that the counting gas already contains methane (CH_4) as a quencher, and so no contamination of the counting gas will occur at the trace levels of our additive. The main advantage is that the absorption of the ^{3}H into the walls and construction materials of the detector is retarded when it is introduced in a form which is tightly bound in such a large molecule rather than, for example, the T_2 or HT molecules. This minimizes the amount of ^{3}H decaying in the walls of the detector and the amount of bremsstrahlung photons entering the chamber. One concern with this species is its relative complexity. The effects on the β-particle energy spectrum due to changes in the tritiated hydrogen molecule are calculable [21–25], due to the simple homonuclear diatomic structure of the molecule and its simple two-electron orbitals. Overlap calculations for the HT decay to HHe are more readily completed than are overlap calculations for the CH_3T to CH_3He decay. Nonetheless, there has been substantial progress in the theoretical and experimental study of the methyl tritium molecule, enabling us to predict the shape of our spectrum. To acquire a working understanding of the possible molecular changes which may affect our spectrum, we will consider the quantum chemistry.

1. Influence of molecular structure on the β-decay spectrum

The methane molecule contains a carbon atom, and four hydrogen atoms. In the tritiated molecule, one or more of the hydrogen atoms is replaced with its unstable heavier isotope, tritium. Chemical considerations are essentially unaffected by the increased mass due to the triton. The molecule may however be affected by the recoil of the daughter ^{3}He atom subsequent to the decay, and by the shaking up of the molecule.

In a formal way, Kaplan and Smutney [21] have described the molecular effects on the decay spectrum through the introduction of an additional factor with the Fermi theory to account for the transitions to the various possible final molecular states. We will define $W_{0\to n}$ as the fractional probability for excitation of the molecule to final state n, where there are $N-1$ discrete final states of excitation and the Nth state is excitation to the continuum (*shake-off*). We also define $\Delta E_{0\to n}$ as the chemical energy given up in a transition from the ground state of the parent molecule to the nth level of excitation of the electron cloud for the daughter molecule. $\Delta E_{0\to n}$ is referred to as the chemical shift. A negative value of $\Delta E_{0\to n}$ indicates energy transferred to the decay products, and Kaplan and Smutney [21] have shown that this chemical shift always transfers energy to the products in the decay of tritiated hydrocarbons. We employ this sign convention for the fragmentation energy taken up in the daughter products in this work. Then we simply rewrite Eq. (1) above as follows:

$$P(E_e)dE_e=\sum_{n=0}^{N} W_{0\to n}[C'F(Z_f,E_e)p_eE_e(E_\nu^n)^2]dE_e,$$

where

$$E_\nu^n=E_0+\Delta E_{0\to n}-E_e.$$

Then upon expanding and squaring E_ν^n, and completing the summation, we may simplify through the use of the mean value of the chemical shift:

$$P(E_e)dE_e=C'p_eE_e[(E_0-E_e)^2+2(E_0-E_e)\cdot\overline{\Delta E}+\overline{\Delta E^2}]\times F(Z_f,E_e)dE_e. \qquad (5)$$

In this last step, we have taken

$$\overline{\Delta E} = \sum_{n=0}^{N} W_{0\to n} \Delta E_{0\to n},$$

$$\overline{\Delta E^2} = \sum_{n=0}^{N} W_{0\to n} (\Delta E_{0\to n})^2.$$

Strictly, this does not correctly describe the shape of the spectrum near the endpoint, where individual final states contribute a *staircase* approach to the axis. For our purposes, with our broad resolution function, and our focus on the lower energy portion of the spectrum, this form of the equation is preferable.

In the near Hartree-Fock formalism, electron orbitals are described with respect to the nuclear coordinates and forces, but without consideration of the mutual repulsions (correlations) between electrons. In addition, since the Hartree-Fock orbitals typically conserve electron spin and orbital angular momentum separately, better predictions are achieved by taking into account spin-orbit coupling through the configuration interaction method. In this way, Ikuta, Iwata, and Imamura [25] have calculated a 61% overlap, upon decay, to the CH_3He^+ ground state, with ~ -50 eV of the decay energy being required to excite the electron cloud and break the CH_3-He bond. Kaplan and Smutney [21] have confirmed these calculations, predicting that 62% of transitions will be to the ground state. Claxton, Schafroth, and Meier [24] have also used similar methods to achieve very precise calculations for the methyl tritium molecule, employing a basis set of 376 spin-adapted configurations (SAC's), yielding $\overline{\Delta E} = -52.10$ eV, after summing over 99.83% of the final states. They predict 59% overlap to the ground state of CH_3He^+, and they provide a detailed prediction of the excitation spectrum of the decay products in their Fig. 1. (Their more ambitious calculation used 2926 SAC's, and yielded $\overline{\Delta E} = -49.5$ eV, with 57.8% transition probability to the ground state, but they provide no detail for the excitation spectrum from this calculation. For our purposes, these small differences are not significant within our resolution, whereas the excitation spectrum from their simpler analysis is of use.) While they have not quoted a value for $\overline{\Delta E^2}$, it may be estimated from their figure to be within 20% of $(\overline{\Delta E})^2$ for the 376 SAC case, thus introducing a small error to the above calculation on making such a substitution. This enables us to use the term $(E_0 - E_e + \overline{\Delta E})^2$ in place of the square-bracketed term in Eq. (5) above. Lippmaa *et al.* [26] have measured the $^3H \to {}^3He$ mass defect as $18\,599 \pm 2$ eV. We initially take this for our E_0, redefining E_e as only the kinetic energy of the escaping β particle. (Audi *et al.* [27] have revised this to $18\,590 \pm 2$ eV in NUBASE, published subsequent to our initial analysis. This difference was found to have no significant effect on our results.) Subsequently ignoring the small uncertainty acquired in substituting $(\overline{\Delta E})^2$ in place of $\overline{\Delta E^2}$, we modify Eq. (5) to describe our spectrum, substituting in place of E_0 the value $E_0 + \overline{\Delta E} = 18\,547$ eV. (In this, we have thus far neglected eventual recovery of any of the excitation energy in ionization of the gas. We call this the neutralization energy, and we will treat this as a shift in the origin of our energy spectrum when analyzing the observations.) Thus, we move beyond the sudden approximation and account for the energy balance of the orbital electrons and the decay products.

The additional energy uncertainties which we have not resolved in our calculations above include the $\leqslant 3$ eV nuclear recoil energy, the ± 2 eV uncertainty in the Lippmaa *et al.* end-point measurement, and the ~ 5 eV (before squaring) uncertainty acquired in the use of $(\overline{\Delta E})^2$ for the final term in the sum in Eq. (5) above.

2. Methyl tritium decays, screening effects revisited

We note that $\overline{\Delta E}$ is significantly greater than the methane bond energy of -18.2 eV, placing our decision to treat the excitation of the orbital electron structure as a perturbation to the β decay in question. Nonetheless Kaplan and Smutney [21] have argued that the ''instantaneity'' of the decay fragmentation and β-particle escape relative to the nuclear recoil justifies this use of perturbation methods for β-particle energies above ~ 870 eV. In the event that the decay results in dissociation of the daughter ^{3}He atom, with the rest of the molecule remaining intact, there are three possible final states:

$$CH_3T \to CH_3^{(*)} + {}^3He^{+(*)} + \beta^- + \overline{\nu_e}, \tag{6}$$

$$CH_3T \to CH_3^{+(*)} + {}^3He^{(*)} + \beta^- + \overline{\nu_e}, \tag{7}$$

$$CH_3T \to CH_3^{-(*)} + {}^3He^{2+} + \beta^- + \overline{\nu_e}, \tag{8}$$

where the superscripts $(*)$ indicate the inclusion of all possible excited states. Snell and Pleasanton [28] have reported that a neutral ^{3}He decay product is observed for 83% of decays and Eq. (6) is almost never observed, despite the self-consistent field (SCF) calculations which predict $\sim 60\%$ overlap to the CH_3He^+ ground state. [All other observed end states were more fragmented, and, Eq. (8) was never observed.] This seeming inconsistency between predictions and observations is acknowledged by Ikuta, Iwata, and Imamura, where they note that this discrepancy must indicate some probability that the CH_3^+ ion is left excited. They have also calculated that there is no minimum in the relationship between the CH_3-He bond energy and the bond length, and that the binding continues to decrease at large distance. This indicates that the molecule will inevitably not accept the ^{3}He daughter. The energy lost to the decay from the breaking of the CH_3-He bond is accounted for in the calculations of Kaplan and Smutney, as well as those of Ikuta, Iwata, and Imamura, and those of Claxton, Schafroth, and Meier, though there are small disagreements (~ 2 eV) in the magnitude of the total chemical energy change.

In the sudden approximation, which we employ to describe the atomic and molecular environment encountered by the decay products, the molecule has not had time to dissociate. Palke and Lipscomb [29] give the occupation number for electrons at the hydrogen atom in methane as 0.867, based on a calculation employing linear combinations of atomic orbitals to produce molecular orbitals [linear combi-

nation of atomic orbitals–molecular orbitals (LCAO-MO) method]. This suggests a minimum screening potential, consistent with the sudden approximation, of $0.867\times 41.7 = 36.2$ eV. Kaplan and Smutney [21] have predicted that the molecular rearrangement is largely local to the decaying ^{3}H atom, and that the electron density at the daughter ^{3}He will increase by 0.915 in the decay. Taking Palke's and Lipscomb's calculations for the CH_4 molecule and increasing this by 0.915 yields a naive estimate of the occupation number for electrons at the ^{3}He daughter of 1.782. In so doing, if we further assume that the increased electron occupation goes directly to the ground state, we predict a screening potential of ~86 eV. On the other hand, if the weightings shown in Table I apply to the total electron cloud at the ^{3}He atom, the screening potential will be 74 eV, and the excitation of the electron cloud at the ^{3}He atom will agree with the Claxton, Schafroth, and Meier calculation of the mean excitation energy to within about two electron volts. The calculations of Claxton, Schafroth, and Meier predict 59% overlap to the ground state of the CH_3He^+ ion, compared with 70% from Table I above for the isolated atom, which supports a greater level of excitation of the molecule than is evident in our naive extrapolation of the Table I calculations into the increased electron density in the decay. However, while the uncertainties mentioned above in Sec. II C 1 pertain to the spectrum end point, the ~5 eV uncertainty acquired in the use of $(\overline{\Delta E})^2$ in place of $\overline{\Delta E^2}$ will also affect V_s. This uncertainty and the eventual neutralization of the decay products preclude distinguishing these small excitation variations from our results. We, therefore, predict a range of screening potentials, V_s, of between 36 and 86 eV, with 74 eV or more being consistent with the SCF calculations of Claxton, Schafroth, and Meier, and 36 eV being consistent with the sudden approximation for the atom alone. The higher screening potentials will also be consistent with the predictions of Kaplan and Smutney of an increased electron density at the decaying atom, and will support an hypothesis that this increased electron density contributes in the calculation of the screening potential. This will then lead to an expectation of a high probability for a neutral ^{3}He atom among the decay products. In this last respect, this will also be consistent with the observations of Snell and Pleasanton of ~83% probability of neutral helium in the final states.

We will, therefore, fit our experimental data to a theoretical β spectrum, where

$$P(E_e)dE_e = C'F(Z_f,E_{es})(E_{0\Delta}-E_e)^2 p_{es}E_{es}\,dE_e. \quad (9)$$

We will use

$$E_{es} = E_e - V_s,$$

and

$$E_{0\Delta} = E_0 + \overline{\Delta E} = 18547 \pm 2 \pm 5 \text{ eV}.$$

where the 2 eV is attributable to Lippmaa *et al.*, and the 5 eV is due to our simplification of $\overline{\Delta E^2}$.

For an isolated ^{3}H atom, the degree of excitation of the daughter ^{3}He electron orbitals is determined as described in Sec. II B 1 above, by the overlap between hydrogen and helium orbitals. In the molecular case, similar overlap calculations using LCAO-MO orbitals predict the degree of excitation of the molecule. The calculation of Claxton, Schafroth, and Meier predicted the mean excitation of the CH_3He^+ molecule, $\overline{\Delta\varepsilon^*}$, as −20.4 eV. This may be compared with −12.7 eV of excitation in the case of the decay of the bare atom alone, as shown in the fourth column of Table I, an absolute increase of ~8 eV. The efficiency for conversion of this excitation energy into ionization in the gas is not precisely determined. It is a function of the electron emission and fluorescence spectra of the daughter products, and the ionization potentials of the components of the gas. Kaplan and Smutney [21] discuss the effects of the β decay on the molecular electron shell. They conclude that the excitation spectra for all organic molecules are similar, exhibiting a single electron transition for approximately half of excited molecules, and multielectron transitions for the remaining cases. This suggests a minimum weighted mean of 0.6 ion pairs liberated on neutralization, which will be registered as 16 eV in the gas. The excitation spectrum is carefully predicted by Claxton, Schafroth, and Meier for the 376 SAC case. Since the lowest excited state in their excitation spectrum is 22 eV above the ground state, and this exceeds the ionization potential for methane molecules, one may make naive predictions of the resulting ionization which will be observed in the spectrometer. Through analyzing this excitation spectrum, we are led to expect neutralization of the products to produce a weighted mean of up to 1.16 ion pairs in the gas, based on the methane ionization potential. At the calibration established for the spectrometer, this would be observed as 30 eV of neutralization energy, offsetting the origin of our β spectrum.

We therefore study the low-energy end of the spectrum, near the limit of the region of validity for Rose's approximation, for evidence of a screening potential V_s, which is closer to 74 eV than to 36 eV. This prediction for the screening potential is guided by theoretical investigations of ^{3}H β decay in the CH_3T molecule, and specifically by the calculations of Claxton, Schafroth, and Meier giving $\overline{\Delta E} = -52.1$ eV and $\overline{\Delta\varepsilon^*} = -20.4$ eV, and the predictions of Kaplan and Smutney of a 0.915 increase in electron intensity at the decaying atom. We also expect our spectrum to be shifted from the analyzer pedestal by between ~16 and ~30 eV due to the recovery of some of the molecular neutralization energy in the gas, simultaneously with the ionization attributable to the β particle.

III. OBSERVATIONS AND ANALYSIS

Our observations were made with a large volume proportional chamber, containing tritiated methane in 90% argon/10% methane ($P10$) counting gas. We discuss our experimental method, and the precision of our apparatus elsewhere [16]. Our characterization of the detector employed two activated K-capture sources (^{37}Ar and ^{79}Kr) mixed in trace amounts into the counting gas, and an external ^{55}Fe x-ray source. The activated sources initiate ionizing showers in the $P10$ counting gas, largely through Auger electron emission

either on decay or in subsequent fluorescence conversions on the argon of the counting gas. The small fraction of remaining fluorescence decays converts easily in the gas, and permits precise determination of two critical characteristics of the detector. Our gas proportional chamber energy resolution was observed to be 14.5% full width at half maximum (FWHM) at the ^{55}Mn $K_{\alpha 1}$ x-ray (5899 eV), and to vary as $E^{-1/2}$ across the spectrum. We have also measured a space charge nonlinearity affecting both the energy axis and the normalization at the fractional level of $2.2\times10^{-5}\pm5\%$ ch^{-1}. An additional fiducial volume dependence on energy was measured, in our β spectra, at the level of $3.7\times10^{-5}\pm7\%$ ch^{-1}. Backgrounds were observed at below 2% of the data rate, and carefully analyzed. A careful background subtraction method is employed, since the measurement of the background spectrum is contaminated by residual ^{3}H outgassing from the chamber construction materials, which affects the observation of the detector live time and may lead to incorrect subtraction of the backgrounds.

A. Background spectra

The dominant components of the backgrounds can be successfully described as originating in three ways. One component of the background is a gently sloping (with energy) distribution resulting from cosmic and other natural radiation. We have also identified some fluorescence features which we believe result from excitation of the gold cathode surfaces by these backgrounds. We also observe a E^{-1} event distribution attributable to bremsstrahlung photons originating within the detector walls, largely from ^{3}H nuclei contaminating these walls.

In determining the actual shape and rate of these background components in order to subtract them from our tritium observations, account was taken of the raw background event rate to be expected in the chamber, exclusive of the residual tritium which outgasses into the detector from the construction materials during a background acquisition experiment. As well, corrections are applied to the magnitude of the background subtraction in order to compensate for the detector dead time which results from our attempts to achieve a high tritium to background event ratio during final spectrum acquisition. The analysis of the backgrounds was conducted as discussed in our prior paper [16].

B. ^{3}H β-decay spectrum

1. Gas gain matching

The necessity to ensure adequate matching of the gas density and gas gain conditions between background data sets and ^{3}H data sets has led us to also record the position of a peak due to our ^{55}Fe source immediately *before* and *after* acquiring background and ^{3}H spectra. For the particular pair of background and ^{3}H spectra to be discussed below, the peaks were observed to be nearly coincident, with the gain for the background spectrum being 0.5% smaller than that of the ^{3}H spectrum. This difference is of the same order as the drift in the peak position during acquisition of the background. To rebin the background spectrum prior to subtraction from the ^{3}H data would require careful management of the uncertainties for each channel of background data, and undoubtedly would slightly increase the uncertainty in this data set. We have considered the value of doing such rebinning for this pair of spectra, and compared the results of such rebinning with the raw background data. It is apparent from the differences between the original background data set, and a rebinned data set, that there is little benefit in rebinning this data. The difference between the two data sets is of order $\sim10-\sim40$ counts per channel over the entire useful range of the data. After subtraction of the ^{3}H contamination of the background spectrum and scaling the balance in order to achieve an *equal live time* subtraction, the difference will be less than ~20 counts per channel, which is trivial relative to the normal deviations in each channel of the 10^8 events of ^{3}H data. In addition, the difference between these two data sets is a smooth function, small compared with and yet similar in shape to the energy dependence in the detector's acceptance. We will disregard this small mismatch in gas gain.

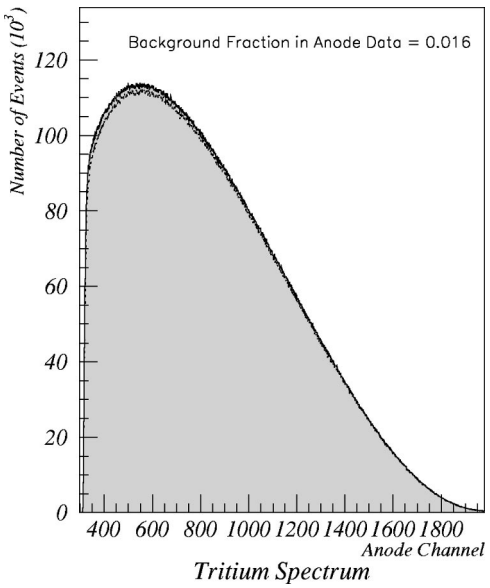

FIG. 1. ^{3}H β-decay spectrum before and after background subtraction.

2. The ^{3}H spectrum

The reduced background shown in our previous paper was subtracted from the ^{3}H spectrum of Fig. 1. The resulting change in the spectrum is barely apparent in the lower energy portion of Fig. 1. The background accounts for less than 2% of the ^{3}H spectrum, and the uncertainties due to the background subtraction were added to those of the ^{3}H data, increasing the ^{3}H statistical uncertainty by less than $\frac{1}{8}\sigma$.

We now compare the observed spectrum to our theoretical predictions, fitting the data to the β-particle energy distribution described in Eq. (9) above. We convolve the theory with elements of our detector's response, allowing for the measured energy calibration nonlinearity of 2.2×10^{-5} ch^{-1} times the energy dispersion (and associated channel width increases), the detector's additional acceptance nonlinearity

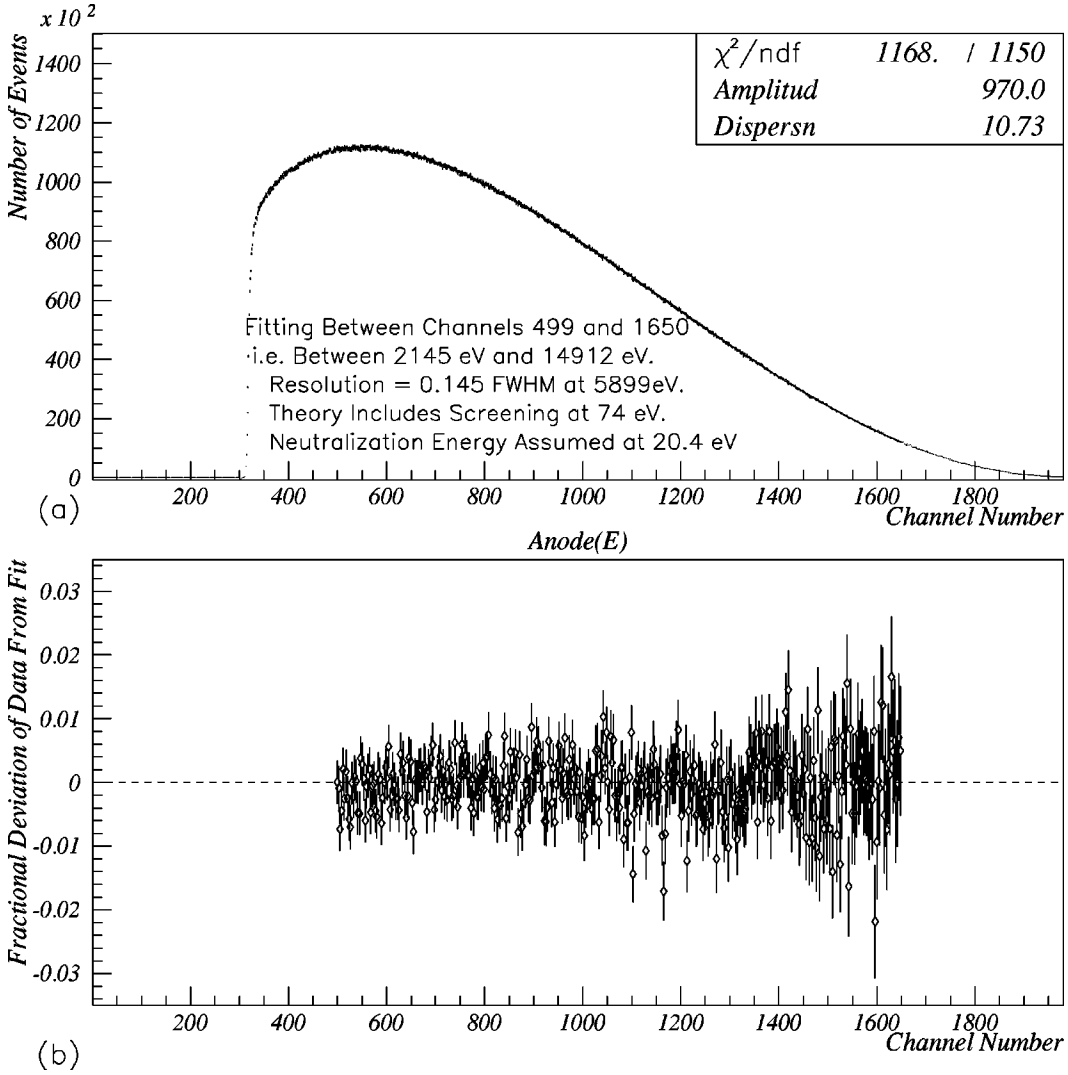

FIG. 2. ^{3}H spectrum preliminary fit results. (a) Fit spectrum. (b) Fractional deviations of data from fit (error bars are $\sim 1\sigma$). For clarity, only one of each three data points is shown.

of 3.7×10^{-5} ch^{-1} times the normalization constant, the wall effects predicted with our Monte Carlo simulations at about $\frac{5}{8}\sigma$ near the maximum in the spectrum, initially using the predicted screening potential and neutralization energy. We fit the spectrum in the higher energy region first, where the wall effects are most pronounced, in order to determine the magnitude of these effects and to verify the systematics of our experiment. Then we fit the lower energy portion of the spectrum, where the shape is most sensitive to screening, in order to better determine the magnitude of the screening potential. Finally, we investigate the consistency of both determined parameters across the combined range in the spectrum, allowing for the neutralization energy, and we iterate the fitting where necessary.

We make our initial fits over the β-particle energy range of 2.14–14.9 keV, assuming the predicted wall effects, a 74 eV screening potential, and -20 eV of neutralization energy. The normalization and energy dispersion are free parameters in these fits. The spectrum has a maximum near 2.5 keV. This fit yields a χ^2 of 1168, for the 1150 degrees of freedom (Fig. 2), or 1.016 per degree of freedom, giving a 34.9% goodness of fit. We have tested the dependence of this fit on the detector's energy resolution, varying the nominal 14.5% FWHM resolution at the ^{55}Mn $K_{\alpha1}$ x ray between 13.0 and 16.0%, without affecting χ^2.

We now look at the influence of the wall effects on the measurement. We have allowed the magnitude of wall effects to be a third free parameter in refitting the data. The refit of the spectrum indicates a higher level of wall effects than we have estimated, by a factor of 2.21. This may be due to difficulties in simulating the interactions of low-energy electrons [30]. The χ^2 from this fit is 1141 units, over the now 1149 degrees of freedom, yielding 56.1% goodness of fit. (For normally distributed deviations, there is a 1% probability of achieving a measured result for which χ^2 $[=\delta^2/\sigma^2 \geqslant 2.58^2] \approx 6.66$ for one degree of freedom [31]. We therefore take an improvement in χ^2 of 6.66, attributed to a change in one parameter, as supporting 99% confidence in the improved value assigned to that parameter over the prior value. In this case, our improvement attributable to the wall

effect parameter is more than four times this.) The region of the fit was the same as for the prior fit, and includes 80% of the 98.4 million ^{3}H events recorded in the spectrum. The improvement in χ^2 of 27 units, due to the introduction of the wall effect parameter, is a strong indicator that event degradation due to wall effects is more prevalent in the observations than we had first predicted, and the effect exceeds 1σ near the maximum in the spectrum.

3. Wall effects vs nonlinear effects

We have investigated the dependence of our fits on the nonlinear corrections which we have applied to our spectrum. The space charge nonlinearity which affects both the normalization and the linearity of the energy axis, has been measured at $2.2\times10^{-5}\,\mathrm{ch}^{-1}\pm5\%$. The additional energy dependence in the fiducial volume was measured at $3.7\times10^{-5}\,\mathrm{ch}^{-1}\pm7\%$, and affects the normalization alone. The combined normalization correction factor for the spectrum is $5.9\times10^{-5}\,\mathrm{ch}^{-1}\pm6\%$. We are also interested in possible correlations between the magnitude of the wall effect and that of the correction due to these nonlinear effects during the fitting, since there is some residual uncertainty in the nonlinear corrections and an apparently large deviation in the wall effect from our expectations. The concern arises because these corrections act in opposite ways upon the higher energy portions of our spectra, and may blow up if improperly constrained in the analysis. We have, therefore, fit the ^{3}H spectrum for wall effect corrections of between zero and four times the Monte Carlo prediction, while varying the combined nonlinear effects between $3.0\times10^{-5}\,\mathrm{ch}^{-1}$ and $9.0\times10^{-5}\,\mathrm{ch}^{-1}$. For each value of the strength of the wall effect correction, we have sought the nonlinear correction which produces a minimum in χ^2, and then sought the strength of the wall effect correction which achieves the minimum χ^2 from all of these tests. The results are shown in Fig. 3. The curves in Fig. 3(a) demonstrate the dependence of the quality of the fits on the nonlinear correction term for these various strengths of wall effects. The solid curve is for a wall effect of two times the Monte Carlo predicted value, while the dot-dashed curve to the left (right) is for a wall correction of zero (four) times the prediction, and the dashed curve is for a wall correction of one (three) times the predicted strength. Clearly from Fig. 3(a), the χ^2 minima at all strengths of wall effects indicate combined nonlinear terms near the $(5.9\pm0.4)\times10^{-5}\,\mathrm{ch}^{-1}$ range which we determined from the measurements discussed in our previous paper. The wall effect indicated in Fig. 3(b) which minimizes χ^2 is 2.21 ± 0.68 (95% C.L.), in agreement with the factor of 2.21 indicated in our refit above. Figure 3(c) demonstrates the minimized nonlinear correction of $5.84\pm0.16\times10^{-5}\,\mathrm{ch}^{-1}$ (95% C.L.), which overlaps the measured value precisely and coincides with the wall effect strength near 2.2 times the Monte Carlo prediction. This statistical analysis of the dependence of the quality of the fit on these two systematic effects yields a more certain determination ($\pm2.7\%$) of the nonlinearities than the $\pm6\%$ systematic uncertainty established through the direct measurements, reflecting the strong dependence of χ^2 on variations in the nonlinearities. We now also have a determination of the wall effect of

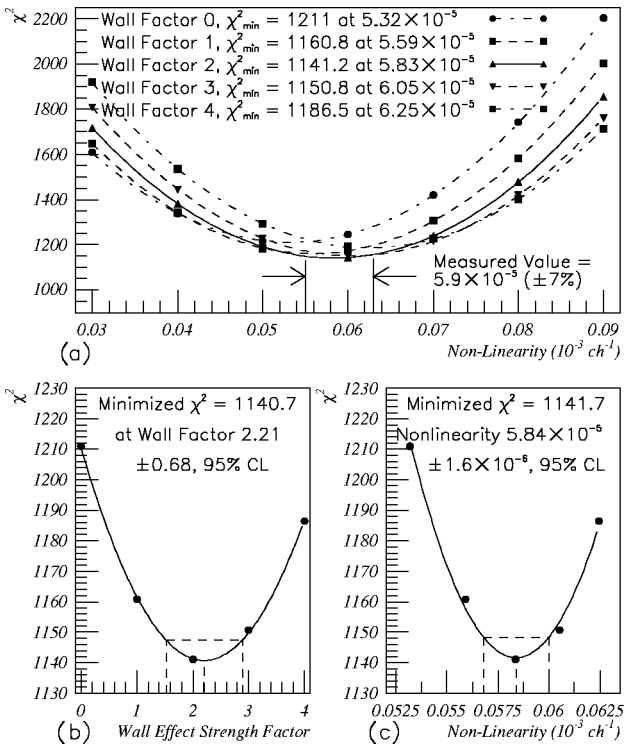

FIG. 3. Nonlinearity and wall effect correlations. (a) χ^2 minima are found for wall effect strengths of between 0 and 4 times the predicted strength, for nonlinearities between $3.0\times10^{-5}\,\mathrm{ch}^{-1}$ and $9.0\times10^{-5}\,\mathrm{ch}^{-1}$. (b) The minima from (a) above are fit to determine the overall minimum at wall effect strength of 2.21 ± 0.68 times the Monte Carlo prediction. (c) The nonlinearity which achieves the minimum in χ^2 is $5.84\times10^{-5}\,\mathrm{ch}^{-1}\pm2.7\%$, which overlaps the measured value.

2.21 ± 0.68 (95% C.L.) times our predicted strength, which is over three standard deviations above our prediction. We believe that this deviation between the prediction and the fit result reflects the fact that angular distributions for low-energy electron scattering are poorly modeled. While this is a significant deviation, it constitutes about a $\frac{3}{4}\sigma$ excursion from expectations near the peak of our ^{3}H spectra, and it is a smooth function. The shape of this distortion tends to supplement those regions of the ^{3}H β-energy spectrum which are most probable, and to deplete the less probable regions of the spectrum.

4. The screening potential

We next test our spectrum for the predicted screening effect. In our initial fits above, we have assumed the theoretically supported 74 eV screening potential, and found significantly improved fits at larger simulated wall effects than our Monte Carlo prediction. However, in this, we have fit the spectrum only above 2.1 keV, in a region which is decidedly less sensitive to the screening effect than is the region below 2 keV. We next test the lower energy region for goodness of fit to various values of the screening potential, while employing the normalization, energy calibration, and wall effect fit parameters found in our refit above.

TABLE II. Low-energy screening potential tests. Results of fitting the observations for screening potentials of between 60 and 95 eV. The wall effect factor used was 2.21 times the Monte Carlo prediction. (The normalizing constant and energy dispersion were held constant.)

Screening potential (eV)	χ^2 (125 ch)	Goodness of fit %
60	247.6	$\ll 0.1$
65	195.0	$\ll 0.1$
70	160.8	1.6
75	145.5	8.4
80	149.0	4.8
85	171.3	0.2
90	212.7	$\ll 0.1$
95	273.2	$\ll 0.1$

In Table II, we show the results for fits between 800 eV and 2.1 keV, for various values of the screening potential. The χ^2 values shown in the table are the totals over the 125 channels employed in our series of screening fits, and the confidence levels demonstrate the goodness of the fits where all of the parameters in the theory have been held fixed.

We have plotted the screening potentials and the χ^2 values of Table II in Fig. 4. The dependence of χ^2 on the screening parameter exhibits a minimum, with the best value for the screening potential being 76.5 ± 3.2 eV (68% C.L.). This result overlaps the 74 eV assumed in fitting the region above 2.1 keV.

Finally, the spectrum was fit over the energy range of 800 eV to 14.9 keV, seeking a simultaneous best fit for five free parameters, those being the normalization, energy dispersion, wall effects, screening potential, and neutralization energy. The fitting (Fig. 5) produces a χ^2 of 1286 units, over 1272 degrees of freedom, indicating by the 38.6% goodness of fit that the deviations between the fit and the observations are randomly distributed. The wall effects concluded from this fit are at a strength of 2.24 ± 0.18 times the Monte Carlo level, in agreement with the above analyses. The corresponding value of the screening potential is 75.7 ± 3.5 eV (68% C.L.), in agreement with our expectations and overlapping the previous results for the 800 eV to 2.1 keV region within

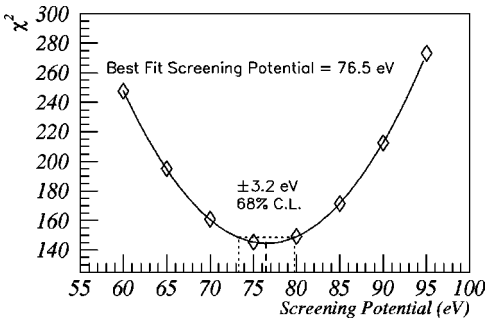

FIG. 4. χ^2 versus screening potential, for screening potentials of between 60 and 95 eV. The minimum χ^2 occurs for a screening potential of $76.5\,\text{eV} \pm 3.2\,\text{eV}$ (68% C.L.).

1σ. The fit also indicates that -22.0 ± 2.6 eV (68% C.L.) of ionization of the counting gas is recovered from neutralization of the decay products. The prediction of Claxton, Schafroth, and Meier was -20.4 eV of excitation, which we expect to produce between 16 and 30 eV of neutralization energy in our spectrometer. We have studied the deviations between the data and the fit function in the region between 800 eV and 2.1 keV, where the spectrum is most sensitive to the screening. The result of this study is consistent with the overall result, with a minimized χ^2 achieved with a screening potential of 76.0 ± 3.2 eV (68% C.L.) in this region.

We have noted a strong anticorrelation between the screening and neutralization parameters over the 23 ± 7 eV range of predicted neutralization values. The ± 7 eV uncertainty in these expectations is not resolved by the small changes in χ^2 produced across this range. We also have a ± 5 eV uncertainty in the neutralization result, due to our $\pm \frac{1}{2}$ channel pedestal uncertainty. We therefore combine these to identify an uncertainty in our neutralization result of ± 9 eV, and through the anticorrelation we also attach this uncertainty to our screening potential result.

We have considered the systematic corrections applied in our analysis, and the possibility that errors in these corrections may bias the results. In the lower portion of Fig. 6, we demonstrate our ^{3}H spectrum at an arbitrary scale. The upper portion of the figure shows those systematic corrections applied in fitting the observations to the Fermi theory. The analysis extends across 1277 of the 1650 data channels (93.4% of the events in the spectrum), from about 800 eV to near 14.9 keV. The cross hatched areas shown were excluded in the analysis. The higher energy excluded region is uncertain for both statistical and systematic reasons, being a region which contains few ^{3}H events, and also a region where systematic effects begin to deviate from the correction algorithms which describe these effects very well elsewhere. The lower energy excluded region contains spectrometer trigger efficiency difficulties, as well as the potential for systematic and intrinsic noise to corrupt our event selection [16]. (This is also the region in which the WKB approximation technique, which is the basis of the Rose approximation, may cease to be applicable.) The solid curves above and below zero demonstrate $\pm 1\sigma$ as a fraction of the background subtracted spectrum. The background fraction, already subtracted, is seen to vary from about 2.5% of the data, down to about half that. The uncertainty contributed by the background subtraction will be $\sim 0.1\%$ or less. The prominent Au L x-ray lines, discussed in our prior paper [16] are apparent near channels 850 and 1050. There is no apparent residue from this subtraction evident in Fig. 5. Wall effects deplete the spectrum at higher energies, and supplement at energies near the maximum in the spectrum. The level of wall effects (shown with the dot-dashed curve), at 2.2 ± 0.7 (95% C.L.) times the predicted level is still small, exceeding σ for the data by a small amount near the maximum in the spectrum, and more substantially at higher energies. Space charge effects, measured at $2.2 \times 10^{-5}\,\text{ch}^{-1} \pm 5\%$, affect the normalization of the spectrometer as well as the linearity of the energy axis. The nonlinear energy scale is shown below the

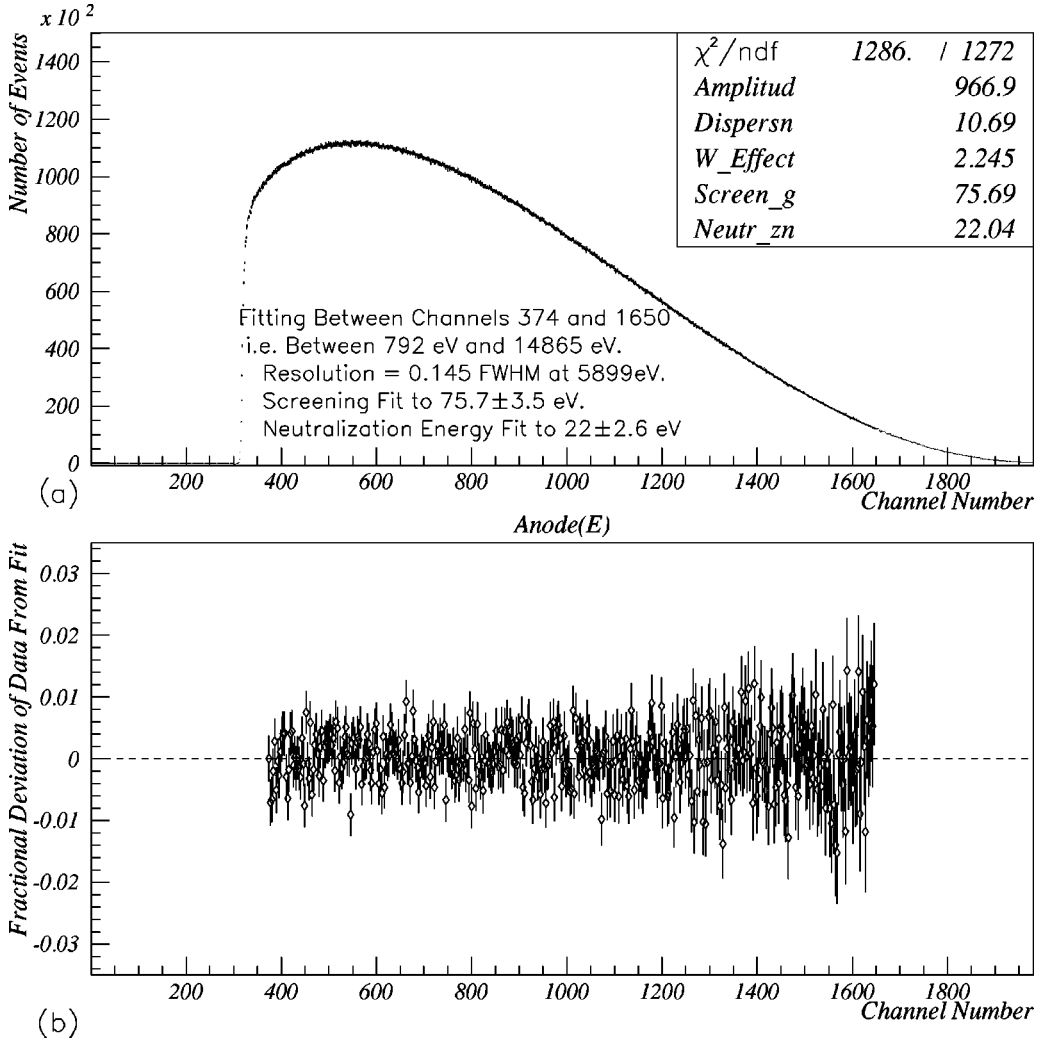

FIG. 5. Final ^{3}H spectrum fit results. (a) χ^2 minimized fit with five simultaneous free parameters (normalization, energy axis dispersion, wall effect strength, screening potential, and molecular neutralization energy). The results are consistent with the wall effect strength determined above, and with the predicted screening potential and neutralization energy. (b) Residual deviations of the data (one out of each three channels shown) from the fit function show no significant systematic structure (normally distributed with a mean of $0.01\pm0.03\sigma$, and a width of $0.99\pm0.02\sigma$).

^{3}H spectrum. The effect is to increase the channel widths of the spectrometer progressively across the range employed for fitting, reaching almost a 3% effect in the highest energy channels. Similarly, a fiducial volume increase with energy of $3.7\times10^{-5}\,\mathrm{ch}^{-1}\pm7\%$ [16] requires correction. Both of these corrections are shown with dotted lines. The effect of the screening potential on the shape of the spectrum is pronounced, as demonstrated by the dashed line indicating the relative shape of the fit function which would result from employing a 0 eV screening potential in this analysis, with all other parameters held fixed at the values which resulted from our fitting. The impact of the 76 eV screening ranges from a 0.2% effect at highest energies, to about 2% at the lowest energies in our fit region. This effect on the shape of the spectrum is dramatically different from that which results from the two normalization corrections, and is comparable to that which results from our full and careful background subtraction. The unexpected increase in the level of wall effects contributes in the lower energy regions at only a small fraction of the strength of the screening potential indicated here.

We therefore find our β spectrum to be well fitted with a screening potential (Fig. 5) of 76 eV. Our 68% C.L. statistical uncertainty is ±4 eV, and our systematic uncertainty is ±9 eV. The simultaneous neutralization energy result is -22 ± 3 (stat) ±9 (sys) eV. This result for the neutralization energy overlaps the -23 ± 7 eV range derived from the work of Kaplan and Smutney [21] and the excitation spectrum of Claxton, Schafroth, and Meier [24]. All other uncertainties in our predictions are at the spectrum end point, and therefore have little impact on these observations of the low-energy portion of the spectrum. These results for the screening and neutralization energies are consistent with the predictions, with our prior conclusion that the wall effect probability is 2.2 ± 0.7 times the Monte Carlo prediction (95% C.L.), and with our measured systematic nonlinearities of $5.9\times10^{-5}\pm6\%\ \mathrm{ch}^{-1}$.

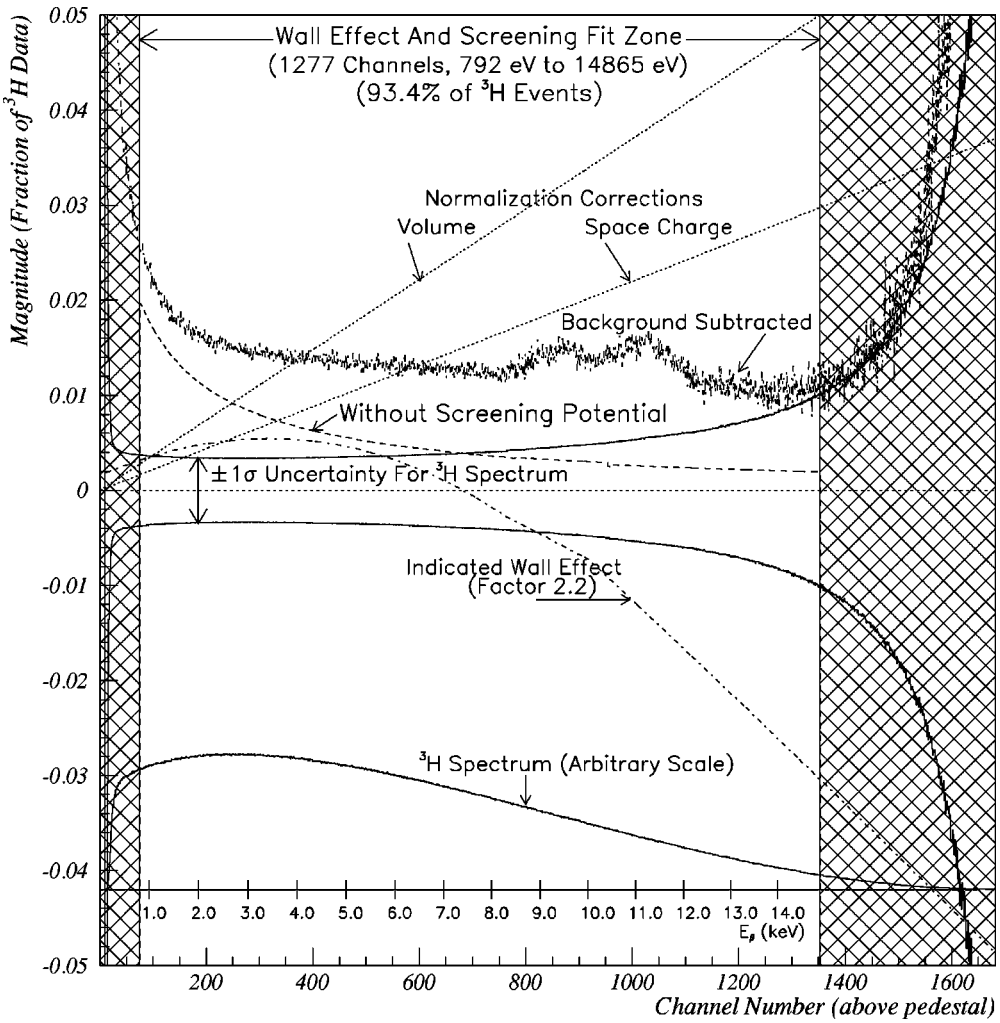

FIG. 6. Magnitude of corrections to the spectrum. The ^{3}H β spectrum is shown at the bottom of the figure, at an arbitrary scale, with the nonlinear energy axis drawn beneath. Factors affecting the fitting are shown as fractions of the background subtracted spectrum. The live time scaled background fraction ranges between about 2.5% and 1% across the spectrum, with the peaks attributed to Au L excitation clearly visible. The wall effect correction is shown (dot-dashed curve) with the shape predicted by our Monte Carlo, but at a level 2.2 times the predicted level, as optimized in the fitting. The measured space charge and fiducial volume dependences on energy affect the normalization in the manner shown (dotted lines). The $\pm 1\sigma$ statistical uncertainty for the spectrum is also shown (solid lines). The fit region contains 93.4% of the $\sim 10^8$ ^{3}H β events collected (after the 1.6% background subtraction). The fits favored a screening potential of 76 eV, concurrently with -22 eV recovered from neutralization of the daughter products. The relative effect of fitting with a 0 eV screening potential is also shown (dashed line).

IV. CONCLUSIONS

We have used the gas proportional chamber technique to study the β-decay spectrum of tritium. This technique is uniquely suited to this measurement because of its good energy resolution (~ 210 eV at 2 keV), its calorimetric nature, and its small corrections for wall effects, and fiducial volume and instrumental nonlinearities. We have observed with certainty, and measured the effect of atomic screening on the energy spectrum from β decays in the tritiated methane molecule.

The standard Fermi theory was used to describe the β-decay spectrum of ^{3}H nuclei. Radiative corrections to the theory were found to be negligible at the level of $\leqslant 10^{-3}$ times the probabilities resulting from the simpler theory. The correction normally made for the screening by the orbital electron cloud on the Coulomb field of the nucleus was incorporated by the Rose approximation. We have predicted the effect of this correction on the atomic ^{3}H β spectrum. We have chosen to observe the decay of ^{3}H in the methyl tritium molecule, and have considered the effects of this molecular environment on the β spectrum.

One concern in our detector is the loss of energy by β particles hitting the walls. The apparatus was designed to operate with a small surface area to gas volume ratio, having a large radius and being run at a high pressure (~ 5 Atm) to keep this effect below $\sim 0.5\%$. This contamination of the β spectrum has been simulated, and it is predicted to be small but not insignificant. The predicted wall effect fraction is less than 0.5% overall, and is 0.25%, or about $\frac{5}{8}\sigma$, for data channels near the maximum in the ^{3}H β spectrum. We have

developed a correction to the spectrum for this effect, which we apply during results analysis. Our observations strongly indicate that wall effects occur at about 2.2 ± 0.7 times this prediction, or about 1% of the data. This produces a distortion of order 1.4σ near the peak of our spectrum, which is about $\frac{3}{4}\sigma$ (0.3% of events) greater than anticipated.

We have studied background contamination of the ^{3}H spectra, which was measured at the level of $\leqslant 2\%$ of our data. The components of the background are well understood, and have been useful in confirming the predictability of the nonlinear space charge effects [16]. This background is easily subtracted from our ^{3}H spectra prior to comparison of our observations with the theory. We have produced ^{3}H spectra, and performed a background subtraction on the collected data. The data has been fit to the theory described, convolved with the systematic effects previously measured and the simulated wall effects.

In fitting the resulting spectra to the theory, the screening correction was incorporated through Rose's technique. We have determined that the observed spectrum is consistent with the theory, on the presumption that the wall effects have been underestimated by the factor determined above.

Our measured β spectrum fits well to a screening potential, due to the final-state orbital electron cloud of the daughter ^{3}He atom, of 76 ± 4 (stat) ± 9 (sys) eV. This is consistent with a high electron occupation probability at the daughter ^{3}He atom in the decay. We simultaneously fit for -22 ± 3 (stat) ± 9 (sys) eV of neutralization energy. Calculations by Kaplan and Smutney [21], Ikuta, Iwata, and Imamura [25], and Claxton, Schafroth, and Meier [24] predict the probability to produce neutral, ground-state products in this decay as $\sim 62\%$, $\sim 61\%$, and $\sim 59\%$, respectively. Our result is consistent with all of these predictions, and suggests that there may be small admixtures of excited neutral or ionized ^{3}He along with excited CH_3^+ or other products in the remaining final states.

[1] A. I. Belesev *et al.*, Phys. Lett. B **350**, 263 (1995).
[2] W. Stoeffl and D. J. Decman, Phys. Rev. Lett. **75**, 3237 (1995).
[3] J. J. Simpson, Phys. Rev. Lett. **54**, 1891 (1985).
[4] A. Hime and J. J. Simpson, Phys. Rev. D **39**, 1837 (1989).
[5] J. J. Simpson and A. Hime, Phys. Rev. D **39**, 1825 (1989).
[6] A. Hime and N. A. Jelly, Phys. Lett. B **257**, 441 (1991).
[7] Bhaskar Sur, Eric B. Norman, K. T. Lesko, M. M. Hindi, Ruth-Mary Larimer, Paul N. Luke, William L. Hansen, and Eugene E. Haller, Phys. Rev. Lett. **66**, 2444 (1991).
[8] I. Zlimen, A. Ljubicic, S. Kaucic, and B. A. Logan, Phys. Rev. Lett. **54**, 1891 (1985).
[9] M. E. Rose, Phys. Rev. **49**, 727 (1936).
[10] S. E. Koonin, Nature (London) **354**, 468 (1991).
[11] D. R. O. Morrison, The Joint Lepton-Photon Symposium and Europhysics Conference on High Energy Physics, Geneva, Switzerland, 1991.
[12] D. R. O. Morrison, Nature (London) **366**, 29 (1993).
[13] S. Weisnagel and J. Law, Can. J. Phys. **67**, 904 (1989).
[14] J. Lindhard and P. G. Hansen, Phys. Rev. Lett. **57**, 965 (1986).
[15] B. Eman and D. Tadić, Phys. Rev. C **33**, 2128 (1986).
[16] D. J. Paterson, C. K. Hargrove, and I. S. Batkin, Nucl. Instrum. Methods Phys. Res. A **425**, 232 (1999).
[17] Heinrich Behrens and Wolfgang Bühring, *Electron Radial Wave Functions and Nuclear Beta Decay* (Clarendon, London, 1982), p.105.
[18] J. M. Blatt and V. F. Weisskopf, *Theoretical Nuclear Physics* (Dover, New York, 1979), p. 682.
[19] I. S. Batkin and M. K. Sundaresan, J. Phys. G **21**, 1061 (1995).
[20] Leonard L. Schiff, *Quantum Mechanics* (McGraw Hill, New York, 1968), p. 94.
[21] I. G. Kaplan and V. N. Smutney, Adv. Quantum Chem. **19**, 289 (1988).
[22] O. Fackler, B. Jeziorski, W. Kolos, H. J. Monkhorst, and K. Szalewicz, Phys. Rev. Lett. **55**, 1388 (1985).
[23] P. Froelich, B. Jeziorski, W. Kolos, H. Monkhorst, A. Saenz, and K. Szalewicz, Phys. Rev. Lett. **71**, 2871 (1993).
[24] T. A. Claxton, S. Schafroth, and P. F. Meier, Phys. Rev. A **45**, 6209 (1992).
[25] S. Ikuta, S. Iwata, and M. Imamura, J. Chem. Phys. **66**, 4671 (1977).
[26] E. Lippmaa, R. Pikver, E. Suurmaa, J. Past, J. Puskar, I. Koppel, and A. Tammik, Phys. Rev. Lett. **54**, 285 (1985).
[27] G. Audi, O. Bersillon, J. Blachot, and A. H. Wapstra, Nucl. Phys. **A624**, 1 (1997).
[28] A. H. Snell and F. Pleasanton, J. Phys. Chem. **62**, 1377 (1958).
[29] W. E. Palke and W. N. Lipscomb, J. Am. Chem. Soc. **88**, 2384 (1966).
[30] F. Sauli, Principles of Operation of Multiwire Proportional and Drift Chambers, Lectures given in the Academic Training Programme of CERN, Organisation Européene pour la Recherche Nucléaire, CERN 77-09, 6, 1977.
[31] Particle Data Group, R. M. Barnett *et al.*, Phys. Rev. D **54**, 1 (1996).